ACS OMEGA

Open Access

http://pubs.acs.org/journal/acsodf

Article

The Thermodynamic Properties of Fat10ylated Proteins Are Regulated by the Fat10ylation Site

Aravind Ravichandran and Ranabir Das*

Cite This: *ACS Omega* 2024, 9, 22265−22276

Read Online

ACCESS | Metrics & More | Article Recommendations | Supporting Information

ABSTRACT: Degradation of proteins by the proteasome is crucial in regulating their levels in the cell. Post-translational modifications, such as ubiquitylation and Fat10ylation, trigger proteasomal degradation of the substrate proteins. While ubiquitylation regulates multiple cellular pathways, Fat10ylation functions explicitly in the inflammatory response pathway. At the proteasome, ubiquitin is recycled after being cleaved from the substrate, while Fat10 is degraded simultaneously with its substrate. Although the thermodynamic properties of the substrate are critical for effective proteasomal degradation, they remain poorly understood for the Fat10-proteasome pathway. We studied the thermodynamic properties of the Fat10∼substrate conjugate to uncover mechanistic details of the pathway. First, the mechanical unfolding of Fat10∼substrate was studied by molecular dynamics simulations, which suggested that the unfolding pathway and unfolding energy of the substrate depend on the site of Fat10 modification. We also investigated different pathways for the entry of the Fat10∼substrate into the proteasome core. Our analysis supports a model where the entry of Fat10, followed by the substrate, is the energetically preferred pathway. Further, we studied Fat10's effect on the thermodynamic properties of distinct substrates, considering their size, flexibility, and surface properties. The results uncovered significant entropic destabilization of substrates due to Fat10ylation, particularly in smaller substrates. For larger substrates, multi-monoFat10ylation is necessary to induce destabilization. Our study further reveals that Fat10 modification at negative patches on substrate surfaces is essential for optimal destabilization and subsequent degradation. These findings provide atomistic insights into the degradation mechanisms in the Fat10 proteasome pathway with potential implications for therapeutic interventions.

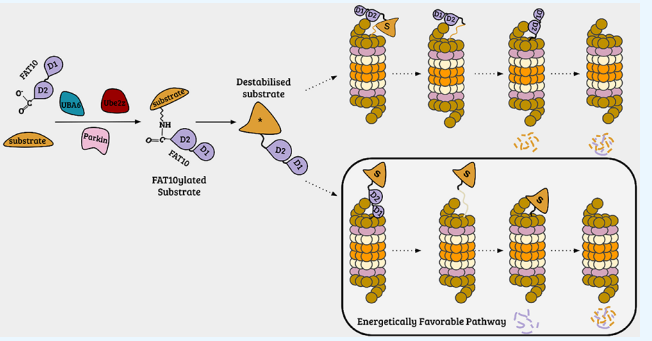

INTRODUCTION

During pathogenic infections, immune cells undergo significant changes in functions like proliferation, proteostasis, antigen presentation, and signaling, which are tightly regulated by the proteasome degradation machinery.[1−4] The proteasome is a 2.5 MDa protein complex comprising the 20S core particle (CP) and the 19S regulatory particle (RP). The CP has a cylindrical structure with narrow entry channels at each end connecting to the central chamber; the RP consists of ATPases and other proteins. Posttranslational modification of substrate proteins with a small protein called ubiquitin targets them to the RP, which removes the ubiquitin tags, unfolds the substrate, and activates CPs for the ATP-dependent degradation of substrates.[5]

Apart from ubiquitin, immune tissues express another ubiquitin-like protein, namely, the human leukocyte antigen (HLA)-F adjacent transcript 10 (Fat10).[6] Posttranslational modification of proteins with the Fat10 tag also targets substrate proteins for degradation. The substrates of Fat10 and ubiquitin are similar,[7,8] suggesting that the Fat10-proteasome pathway is an additional mechanism the immune cells utilize to remodel the cellular conditions. Fat10 includes two ubiquitin-like domains, whose sequence identities with ubiquitin are 29 and 36%.[6] Although each domain has a ubiquitin-like fold, its thermodynamics and surface properties are distinct from ubiquitin.[7] The mechanism of proteasomal degradation of Fat10 substrates differs from that of ubiquitin substrates. Ubiquitin is cleaved from the substrates at the RP by deubiquitinases and recycled to the cellular pool, while Fat10 is degraded along with the substrate.[9]

While the interactions of the polyubiquitin-conjugated substrate and proteasome are well understood, details of interactions between the Fat10-conjugated substrate and the proteasome remain vague. For example, it is unclear if Fat10 enters the proteasome first or the substrate (Figure 1). Substrates must be unfolded and translocated into the core for

Received: February 13, 2024
Revised: April 24, 2024
Accepted: April 29, 2024
Published: May 13, 2024

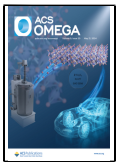

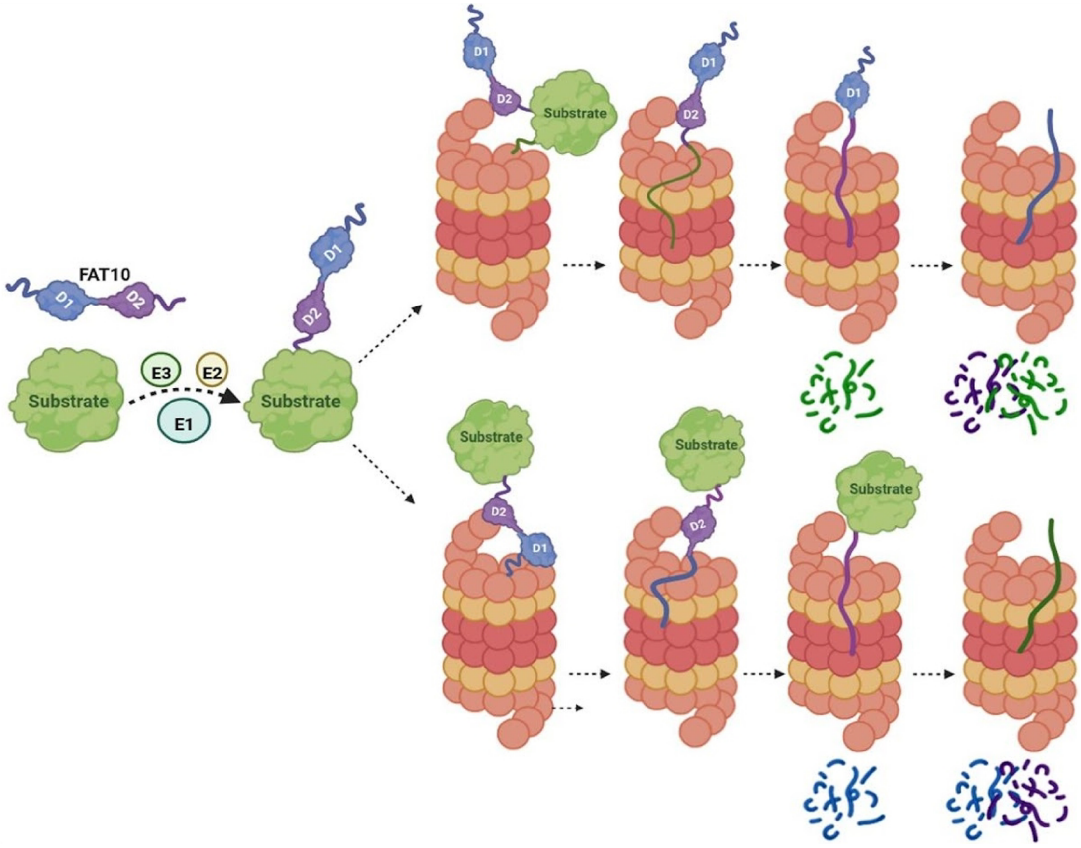

Figure 1. Schematic representation of the probable Fat10-mediated degradation pathways. Fat10 binds to the receptors of the proteasome, and the substrate enters the core particle (top panel). Alternatively, Fat10 might enter the core particle first and be followed by the substrate (bottom panel).

degradation. ATPase associated with RP engages with the substrate and linearizes it by mechanical force, causing it to unfold. An extended N-terminal disordered region in Fat10 is critical for the degradation of Fat10 substrates,[10] suggesting a theory where after RP recognizes the Fat10ylated substrate, the Fat10 N-terminus engages with the ATPase (Figure 1, bottom). However, the theory lacks any structural or in vitro biochemical data. Moreover, the size of the N-terminal disordered region is not conserved in mammals, creating ambiguity about whether the mechanism is conserved across species. It is equally likely that Fat10 binds to receptors in the 19S subunit, and the substrate engages with the ATPase (Figure 1, top). In both situations, the Fat10-substrate conjugate undergoes mechanical unfolding. However, sequential unfolding events during this process are poorly understood.

For the mechanical unfolding of substrates by ATPase, disordered regions in the substrate need to engage with the ATPase. Recent studies uncover that apart from targeting the substrate to RP, the ubiquitin tag partially destabilizes the substrate and creates disordered regions.[11,12] However, well-folded ubiquitin substrates need accessory ATPases like p97 to create disordered regions before they engage with the proteasome.[10] Interestingly, these accessory unfoldases are dispensable for the Fat10-proteasome pathway, suggesting a more profound effect of Fat10 on the substrate structure.[7] We recently reported that Fat10 modulates the thermodynamic stability of substrates to create partially disordered regions.[13] However, substrates with different structures, flexibilities, sizes, and surface charge properties are Fat10ylated and degraded by the proteasome. It remains unclear how Fat10 destabilizes and creates disordered regions on various substrates with different structural properties.

We conducted steered molecular dynamics to study the stepwise mechanical unfolding of Fat10 by proteasome ATPase. Our analysis revealed that pulling from the C-terminus unfolds Fat10 faster than pulling from the N-terminus. We then studied the mechanical unfolding of a Fat10 substrate domain, the Parkin-Ubl domain, which indicated that Fat10 conjugation at the loop regions of the substrate accelerates the substrate unfolding. To study how substrate properties influence Fat10-induced changes in conformational entropy (disorder), we used multiple Fat10-conjugated substrates. We selected three Fat10 substrates with different sizes, surface properties, and inherent flexibilities. The Parkin-Ubl domain, Ube2z (USE1) enzyme, and 40S ribosomal protein s15a are substrates of Fat10,[8,14,15] and they were chosen for this study. The Ubl domain of Parkin is a small, 9 kDa protein. The sizes of s15a and Ube2z are 20 and 25 kDa, respectively. Although Ube2z and s15a have similar dimensions, their surface properties differ, allowing us to probe the effect of Fat10-substrate interactions on the thermodynamic stability. Additionally, to understand the site-specific impact of Fat10ylation, we simulated the Fat10-substrate complex at three lysines located in distinct secondary structures. Our comprehensive analysis provides detailed insights into the effects of Fat10ylation on substrate thermodynamic stability and conformational flexibility.

https://doi.org/10.1021/acsomega.4c01396
ACS Omega 2024, 9, 22265−22276

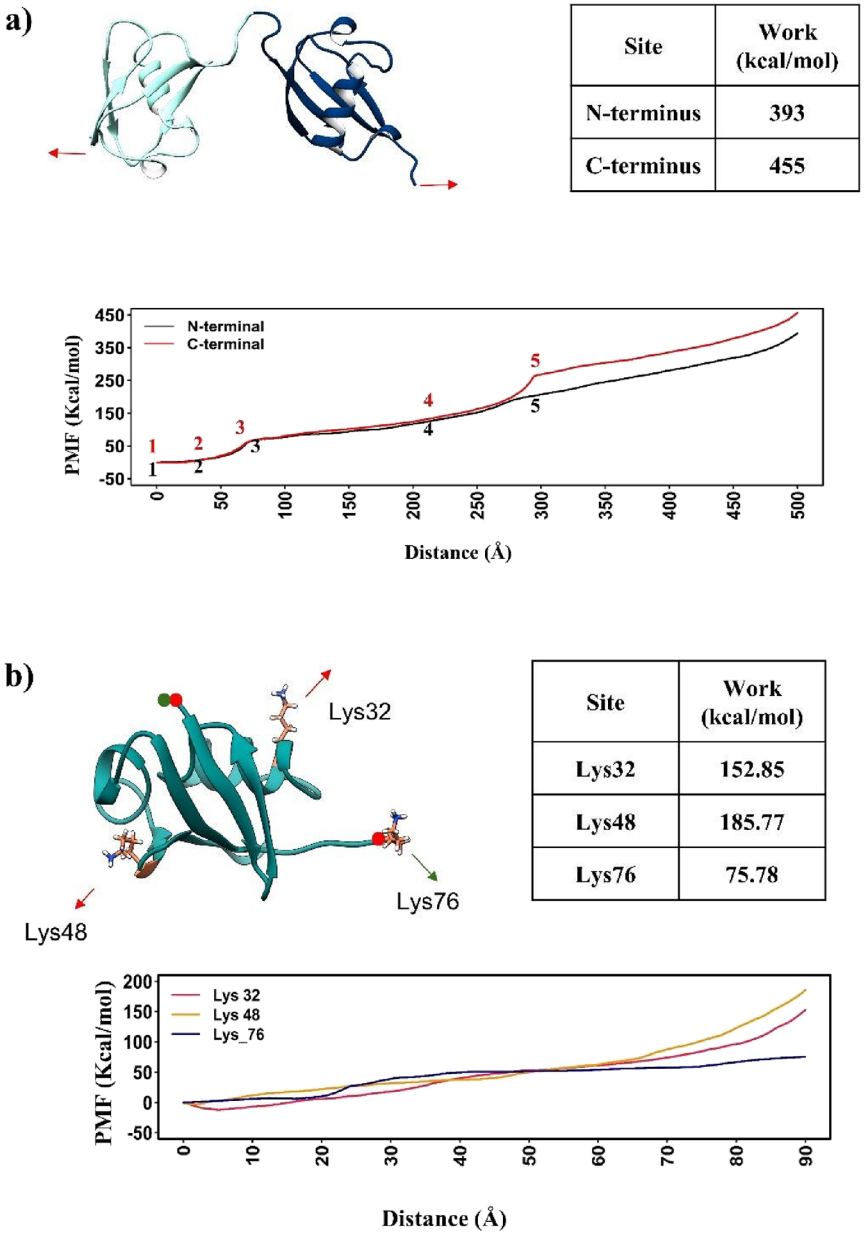

Figure 2. (a) Replication of unfolding mechanism of Fat10 in the proteasomal complex through N-terminal pulling and C-terminal pulling by ASMD. The potential mean force (PMF) is plotted against the normalized end-to-end distance, and the work required to unfold Fat10 is given in a table. (b) The possible lysine side chains of Fat10 modification in the substrate Parkin-Ubl were selected for pulling simulations. Arrows indicate the lysine side chain, and circles denote the residues restrained. For K32 and K48, both the N- and C-termini were restrained, whereas for K76, the N-terminus was retrained. The potential mean force (PMF) is plotted against the normalized end-to-end distance, and the work required to unfold Parkin-Ubl is given in a table.

RESULTS

Unfolding of Fat10 at the Proteasome. To investigate the process of Fat10 unfolding at the proteasome, we conducted adaptive steered molecular dynamics (ASMD) simulations. Previously, we have used bidirectional pulling to study the stabilities of Fat10 and ubiquitin.[13] For studying mechanical unfolding by proteasome ATPase, which linearizes by pulling at one end, examining the Fat10 unfolding by unidirectional pulling is appropriate. Previous work on mechanical unfolding of ubiquitin-like proteins has shown that a constant velocity of 10 Å/ns is slow enough to identify the unfolding intermediates.[16] Therefore, a 10 Å/ns pulling velocity was used to pull Fat10 from either its N-terminal or C-terminal end while keeping the other end restrained. The work required to unfold Fat10 was 393 kcal/mol when pulled from the N-terminus (Figure 2a). Initially, the unstructured regions such as the N-terminal tail, C-terminal tail, and linker between the domains were linearized (Figure S1). Subsequently, the long-range hydrogen bonds between β1-β5, β1- β2, β2-α1, β3-β5, β3-β4, and α1 of D1 disrupted sequentially (Movie S1). The D2 unfolding followed a similar pattern to D1, with β1-β5 unfolding first, followed by β1-β2, β2-α1, and β3-β4. α1 extended subsequently, and finally, the interactions between β3-β5 were lost.

Fat10 required 455 kcal/mol to unfold by mechanical pulling from its C-terminus. Initially, unstructured regions such as the N-terminal, C-terminal, and linker regions were

https://doi.org/10.1021/acsomega.4c01396
ACS Omega 2024, 9, 22265−22276

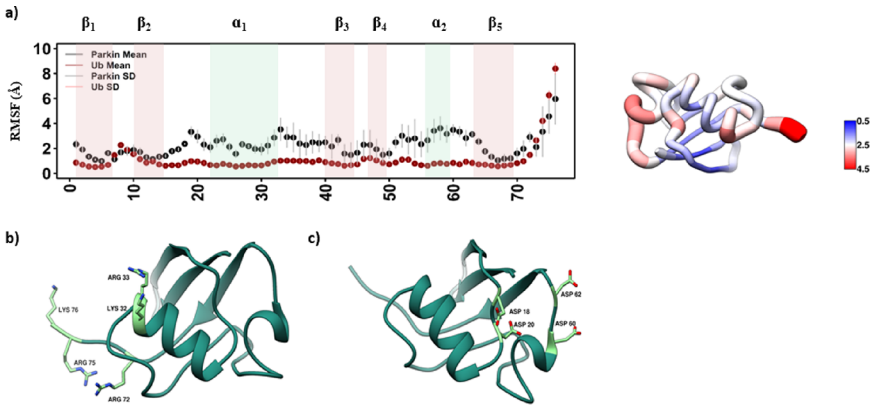

Figure 3. (a) The Cα-RMSF values of the Parkin-Ubl domain are plotted as black-filled circles, and those of ubiquitin are plotted as brown circles. The structure of Parkin-Ubl is shown on the right as a ribbon. The width of ribbons and their color are proportional to the Cα-RMSF values. (b) Positive and (c) negative patches of amino present at flexible regions in the UBL domain of Parkin are highlighted.

linearized (Figure S2). Subsequently, β1 and β2 strands unfolded. The helix α1 dissociated from the core, disrupting the hydrogen bonds between β3 and β5. The entire D2 domain then unfolded, accompanied by the loss of β3-β4 contacts and the unfolding of α1. After the complete linearization of D2, the D1 domain unfolded in a similar pathway (Movie S1). β1 and β2 regions, along with α1, dissociated from the core of the protein, resulting in the unfolding of β3-β5, β3-β4, and α1 within D1. These unfolding pathways of D2 and D1 domains are comparable with sequential dissociation and linearization of secondary structures followed by complete global unfolding. The PMF profile obtained from pulling the C-terminus of Fat10 differed from the N-terminal pulling. This could be because the N-terminal domain of Fat10 is more stable than its C-terminal domain.[13] When the pulling force was applied at the C-terminus, the N-terminal domain was distant and more resistant to unfolding. Alternately, the C-terminal domain unfolds effortlessly, regardless of whether the pulling force is applied at the N- or C-terminus.

The Fat10 Conjugation Site Determines the Substrate's Mechanical Unfolding Pathway. The substrates are conjugated at lysine side chains with the C-terminal end of Fat10.[7] Post entry of Fat10 into the core of proteasome, the substrate will be pulled through the lysine to which Fat10 C-termini were conjugated. The substrate protein's free energy landscape allows multiple unfolding pathways. Mechanical pulling at different lysines can trigger different unfolding pathways in the substrate.[17] Parkin is an E3 ligase for Fat10, and Fat10ylation of Parkin targets it for proteasomal degradation.[14] We chose the Ubl domain of Parkin as a model protein and studied its unfolding pathways by individually pulling at three distinct lysine amino acids located in different secondary structures. The lysines are situated in the C-terminal flexible tail, the short β-strand β4, and the helix α1. The potential mean force (PMF) analysis of the pulling process revealed that when pulling from the C-terminal lysine, the domain provided the least resistance and required the least amount of work to unfold (76 kcal/mol) (Figure 2b). Pulling the substrate from the other lysine residues resulted in approximately double the amount of work needed for unfolding (153 kcal/mol). K48 is located in β4 and is well packed against the short helix α2. Pulling from K48 required the highest amount of work (186 kcal/mol). Overall, the domain provided the greatest resistance when it was pulled from the lysines on β-strands that are well packed against other secondary structures or loops. Interestingly, Fat10 conjugation sites are primarily found in helices and disordered regions in the substrates (Figure S3), which correlates with the pulling simulations.

When Parkin-Ubl was pulled from Lys32, the unfolding process started with the disruption of backbone interactions between β3-β5, followed by β1-β2 and β1-β5 (Figure S4a,b). Subsequently, the α-helix unfolded, and contacts between β3 and β4 disrupted, ultimately resulting in the complete unfolding of the protein. Notably, the region where the pulling force was applied did not necessarily coincide with the primary unfolding region, indicating a complex unfolding pathway. In contrast, when pulling from Lys48, the initial unfolding was initiated by the dissociation of β3-β4 from the core of the protein (Figure S5a,b). This was followed by the dissociation and linearization of the α-helix and subsequent loss of contacts between β1-β5. The entire protein was then linearized as unfolding progressed. Last, when pulled from Lys76, the entire protein core dissociated from β1 (Figure S6a,b), leading to the subsequent linearization of β1 and β2. The α-helix then unfolded, and contacts between β3 and β5 were lost. Finally, the entire protein was linearized. The data highlight distinct unfolding pathways depending on the starting point of the pulling force, demonstrating that different lysine attachment sites can lead to unique unfolding patterns during the mechanical unfolding of the substrate.

Parkin-Ubl Is Significantly Destabilized upon Fat10ylation. We then studied the effect of Fat10lytion on substrate thermodynamics using the Parkin-Ubl domain as the substrate. Although Parkin-Ubl and ubiquitin have the same size and fold,[18] Parkin-Ubl has higher Cα-RMSF values than ubiquitin, suggesting high inherent conformational flexibility in the native structures (Figure 3a). The higher flexibility in the Parkin-Ubl domain may be attributed to two clusters of similar charges that are close in space. Lys32 and Lys33 are present in the helix α1 C-terminal end, and Arg72, Arg75, and Lys76 are present at the C-terminal tail of the domain (Figure 3b). These positively charged residues are in proximity and can create repulsive forces to enhance flexibility in the α1β3 loop. Similarly, Asp18 and Asp20 are present in the β2α1 loop and Asp60 and Asp62 are present in the α2 loop (Figure 3c). These negatively charged residues, clustered close in space, have repulsive interactions that prevent the tight packing of regions around α2 and may be responsible for their high fluctuations.

https://doi.org/10.1021/acsomega.4c01396
ACS Omega 2024, 9, 22265−22276

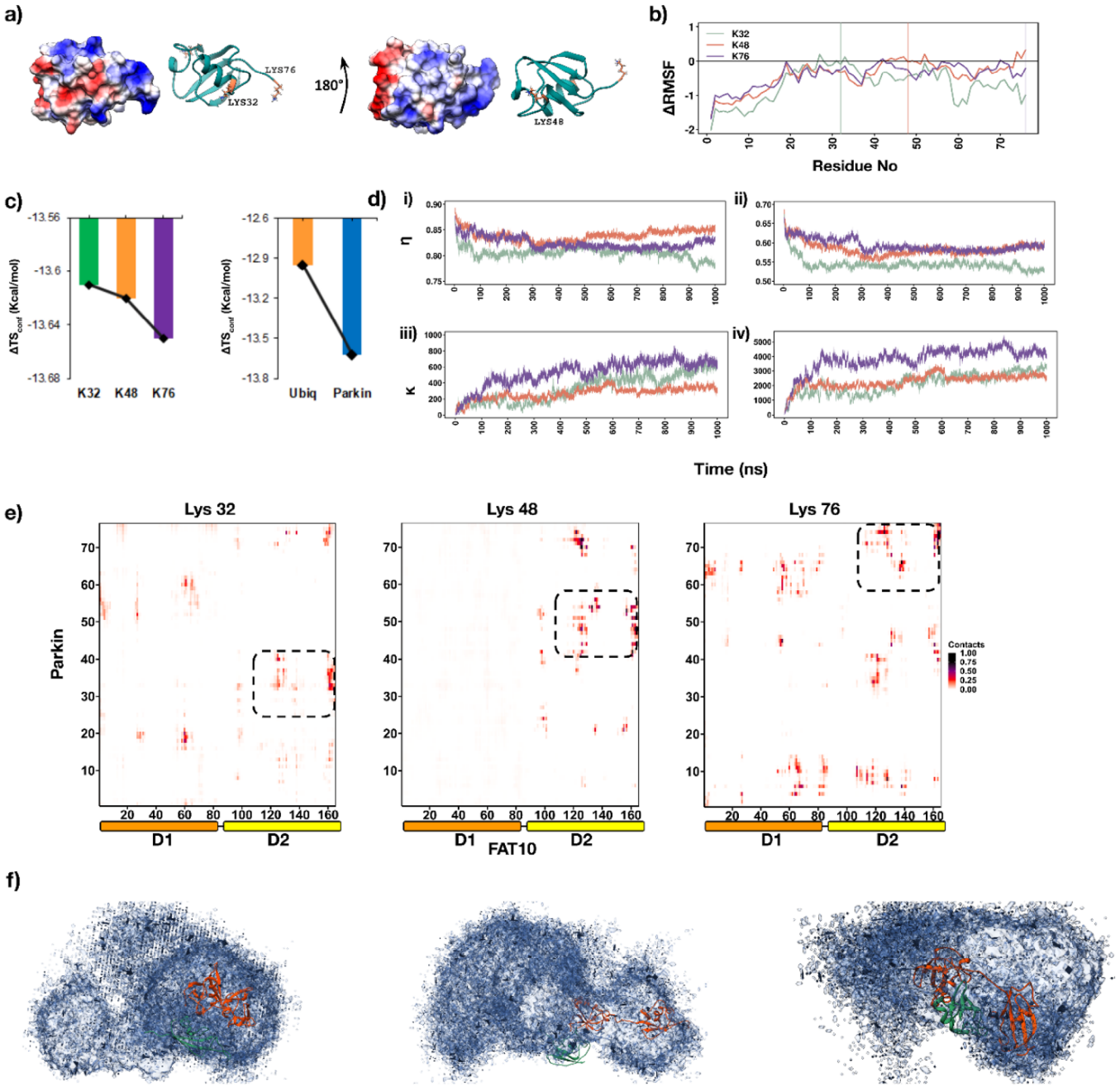

Figure 4. Effect of Fat10 on Parkin-Ubl. (a) The Parkin-Ubl domain surface is colored by the surface electrostatic distribution. The three sites of Fat10 conjugation are shown. (b) ΔRMSF ($RMSF_{unmodified} - RMSF_{Fat10ylated}$) values of Fat10 are plotted against the residues. (c) The conformational entropy ΔTS_{conf} normalized by the number of residues in the substrate is plotted for the three sites, where $\Delta TS_{Fat10ylation} = \Delta TS_{Substrate\sim Fat10} - (\Delta TS_{Fat10} + \Delta TS_{Substrate})$ (left). Ub and Fat10 were conjugated to Parkin UBL at K48, and conformational entropy was plotted (right). (d) Fraction of native contacts (η) plotted as a function of time for (i) Ubl backbone atoms. (ii) Same as (i) but for side-chain atoms. (iii) Fraction of non-native contacts (κ) plotted as a function of time for Ubl-Fat10 backbone interaction. (iv) Same as (iii) but for side-chain atoms. (e) Contact maps plotted for the intermolecular contacts between Fat10 and Ubl for all three sites. The area within the broken black lines shows contacts near the Fat10ylation site. (f) The occupancy of Fat10 in the Parkin-Ubl~Fat10 conjugate is plotted. The Parkin-Ubl molecule is green, and Fat10 is colored orange. Ubl was kept fixed, and the occupancy of Fat10 around Parkin is shown in blue.

The three lysines in the Parkin-Ubl domain that may be modified with Fat10 are Lys32, Lys48, and Lys76. Lys32 is on the central α-helix, Lys48 on the β-sheet β4, and Lys76 at the C-terminal tail (Figure 4a). We initially analyzed the difference in per residue fluctuation between the Fat10ylated and unmodified substrates, termed ΔRMSF (ΔRMSF = $RMSF_{unmodified} - RMSF_{Fat10ylated}$). Negative values of ΔRMSF suggest increased backbone fluctuations upon Fat10ylation. The ΔRMSF values revealed a substantial increase in Parkin-Ubl's fluctuation due to Fat10ylation, regardless of the modification site (Figure 4b). Long-range effects in the substrate were detected in regions far from the conjugation site. Notably, the N-terminal region was stable in the native protein but was significantly destabilized upon Fat10ylation.

To study the effect of Fat10ylation on the conformational ensemble of the substrate-Fat10 conjugate, we calculated per

https://doi.org/10.1021/acsomega.4c01396
ACS Omega 2024, 9, 22265−22276

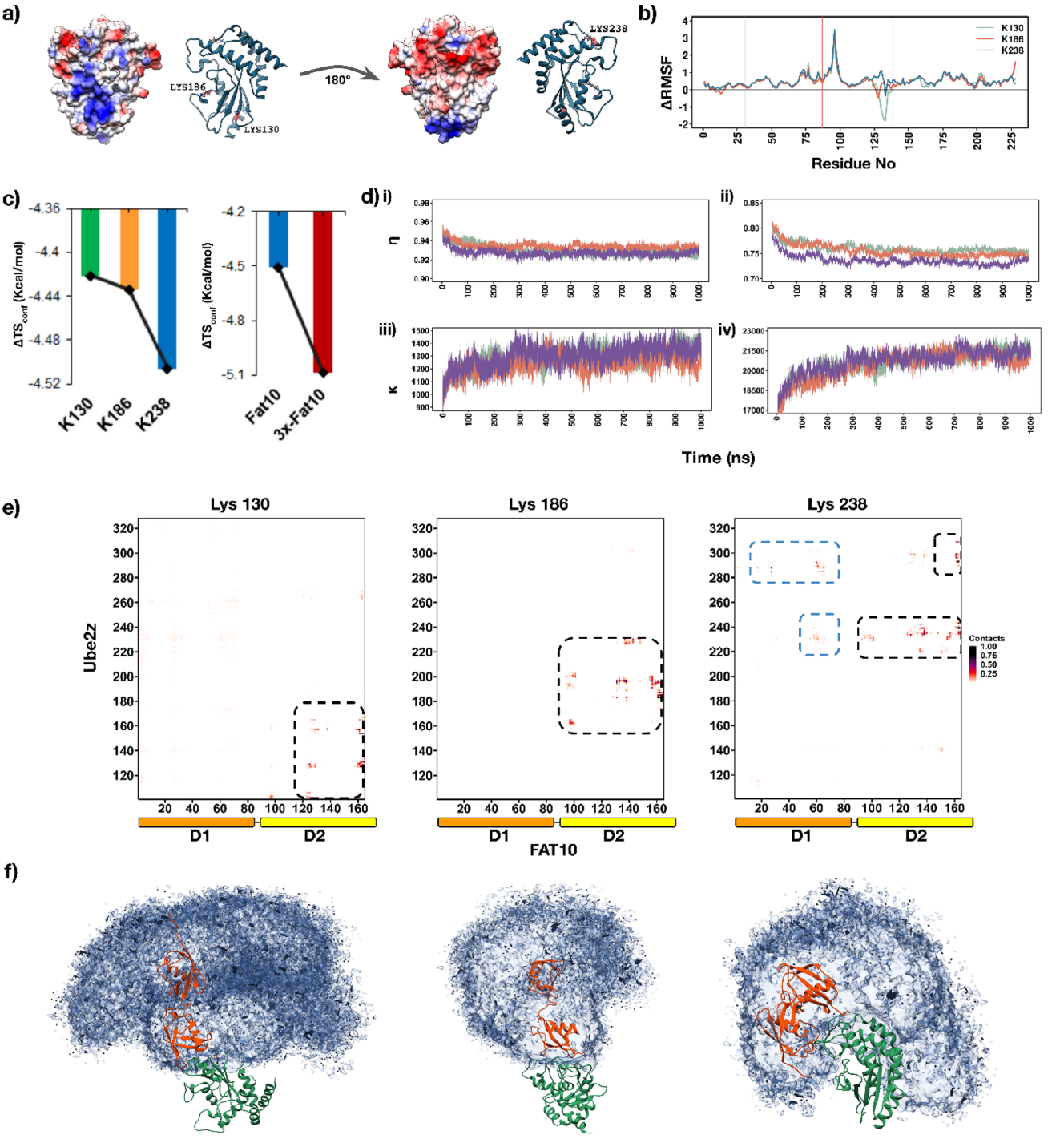

Figure 5. (a) Surface representation of the Ube2z domain is shown, colored by the electrostatic potential. The three lysine residues used for Fat10 conjugation are shown. (b) The ΔRMSF values of Ube2z are plotted. (c) The conformational entropic contributions to the free energy are plotted for the three sites (left). ΔTS_{conf} was also plotted for Ube2z∼Fat10 and Ube2z∼3x(Fat10) molecules (right). (d) Fraction of native contacts (η) plotted as a function of time for (i) Ube2z backbone atoms. (ii) Same as (i) but for side-chain atoms. (iii) Fraction of non-native intermolecular backbone contacts (κ) plotted as a function of time for Ube2z-Fat10 backbone interaction. (iv) Same as (iii) but for side-chain atoms. (e) Contact maps plotted for the intermolecular contacts between Fat10 and Ube2z for all three sites. The broken black lines show contacts near the Fat10ylation site. The broken blue lines show the contacts between the D1 domain and the substrate. (f) The occupancy of Fat10 in the Ube2z∼Fat10 conjugate is plotted. The Ube2z molecule is green, and Fat10 is colored orange. Ube2z was kept fixed, and the occupancy of Fat10 around Ube2z is shown in blue.

residue quasi-harmonic conformational entropy using the covariance matrix of the trajectory. We compared the contribution of entropy to the free energy of the conjugated complex $\Delta TS_{Fat10ylation} = \Delta TS_{Substrate\sim Fat10} - (\Delta TS_{Fat10} + \Delta TS_{Substrate})$ of the Parkin-Ubl∼Fat10 conjugate relative to the sum of entropies in the unmodified substrate and Fat10. A negative ΔTS_{conf} contributes to the overall destabilization of the system. The ΔTS_{conf} values revealed significant destabilizing in the conjugate (Figure 4c). The ΔTS_{conf} values are similar

https://doi.org/10.1021/acsomega.4c01396
ACS Omega 2024, 9, 22265−22276

between all three sites, and Lys76 Fat10ylation showed the highest destabilization effect.

Free energy measurements of substrates attached to either Fat10 or ubiquitin indicated that Fat10 destabilizes substrates greater than ubiquitin.[13] We compared the effects of Fat10 and ubiquitin on the Parkin-Ubl domain. ubiquitin was conjugated to Parkin-Ubl at Lys48 and simulated for 1 μs. The conformational entropy between the Ubl-Ub and Ubl-Fat10 conjugates was then compared. The difference in conformational entropy of the Ubl-Ub conjugate was lower, suggesting that Fat10ylation introduces higher conformational entropy than ubiquitin (Figure 4c). Although Parkin-Ubl and ubiquitin are similar in size, the Cα-RMSF values demonstrate that the inherent flexibility in ubiquitin is lower than that in Parkin-Ubl. We used ubiquitin as a model substrate to assess whether the conformational entropy change depends on the substrate's intrinsic flexibility and compared the Ub-Fat10 conjugate and Ubl-Fat10 conjugate. The Ub-Fat10 conjugate has a lesser change in entropy (−1.4 kcal/mol) than Ubl-Fat10 (−13.6 kcal/mol), suggesting that flexible substrates may have a higher change in entropy upon Fat10ylation.

Although Fat10 introduces higher conformational entropy in the substrate-Fat10 conjugate, it remains unclear whether Fat10 affects the structure and fold of the substrate. To measure changes in the substrate due to Fat10ylation, we examined the native contacts (η) in Parkin-Ubl over time for both backbone (Figure 4d(i)) and side-chain (Figure 4d(ii)) atoms. We also analyzed the transient contacts (κ) between the substrate and Fat10 (Figure 4d(iii),(iv)). Upon Fat10ylation of Parkin-Ubl at Lys76 and Lys48, there was a 15% loss of backbone native contacts, whereas Lys32 modification resulted in a 20% loss of backbone native contacts. Similarly, Lys76 and Lys48 modifications showed a 40% loss in side-chain native contacts, while Lys32 showed a 45% loss in side-chain native contacts. Concurrently, significant non-native contacts formed between the substrate and Fat10 (Figure 4d(iii),(iv)), suggesting that the non-native contacts between Fat10 and the substrate may compete with the native contacts. To gain further insights into the sites of non-native interactions, we generated contact maps as a sum of native and non-native contacts (Figure 4e). The contact maps revealed that Fat10 interacts with the substrate by its C-terminal-conjugated tail, D1 domain, and D2 domain.

To inspect the interactions between Fat10 and the substrate, we plotted the occupancy map of Fat10 obtained from the trajectories (Figure 4f) and representatives from three major clusters (Figure S7). Fat10 created an envelope around the Parkin-Ubl domain with multiple interactions occurring with the Ubl β-sheets. Fat10 conjugated to Lys76 had the most intermolecular interactions with the substrate. Fat10's flexibility to move across the protein surface is limited in the case of Lys32 and Lys48 conjugation, as these sites reside within rigid secondary structures. Conversely, Lys76 is situated in the flexible tail, allowing greater conformational freedom for Fat10 to interact with the substrate. We also calculated pairwise residue interaction energy between Parkin and Fat10 (Figure S7d−f). Positive energy in these plots suggests an unfavorable interaction, while negative energy shows a favorable interaction. The energy plots show several regions with high positive energies for all three conjugating sites, suggesting unfavorable interactions that destabilize the substrate. In summary, Fat10ylation increased the conformational entropy of the flexible substrate Parkin-Ubl domain. Fat10 makes multiple nonspecific interactions with the substrate, disrupting native contacts and destabilizing the native state of the protein.

The Effect of Fat10ylation in Ube2z Is Lower than Parkin-Ubl. Parkin-Ubl is a small, 9 kDa protein. To study the effect of Fat10 on a larger substrate, we chose Ube2z, the conjugating enzyme that forms a thioester bond with Fat10 before transferring it to the substrate.[19,20] Ube2z's activity is regulated by autoFat10ylation, which targets itself for proteasomal degradation.[15] Ube2z is 354 amino acids long. The initial 100 amino acids and the last 27 amino acids are intrinsically disordered regions, which were truncated in our simulations. With 228 amino acids and around 25 kDa, Ube2z was much larger than Parkin-Ubl. Three lysines were chosen for Fat10 conjugation: Lys130, Lys186, and Lys238. Lys130 is located in the β4 β-strand, Lys186 in the β4-α2 loop, and Lys238 in the α5 helix (Figure 5a). Ube2z is mostly rigid compared with Parkin-Ubl (Figure S8). There are three regions with relatively higher flexibility in Ube2z. The loop between β4 and α2 and the loop between α2 and α3 regions in the UBC domain of Ube2z demonstrate the highest fluctuations compared to other regions. Previous studies have identified the β4α2 loop as a highly fluctuating region in various E2 enzymes.[21−23]

We repeated the measurement of the conformational entropy of the conjugates where Fat10 is conjugated to the three lysines. The ΔRMSF profile shows an overall negligible change (Figure 5b), indicating no effect on local fluctuations upon Fat10ylation. Noticeably, Fat10ylation at any of the three sites stabilized the active site loop. Allosteric modulation of the active site loop dynamics plays a prominent role in E2 activity.[21] Fat10lytion-induced changes in Ube2z activity are intriguing subjects for future research. All the conjugates showed negative conformational entropy (∼4.4 kcal/mol per residue) (Figure 5c). There was no significant difference in the conformational entropy values across the sites. For the larger substrate Ube2z, the change in conformational entropy was lower than that for the smaller substrate Parkin-Ubl. Polymers of Fat10 have not been detected on substrates as yet. However, Fat10 may be conjugated to multiple lysines on substrates, leading to multi-monoFat10ylation.[24] For larger substrates with multiple lysines available, multi-monoFat10ylation may be beneficial to create enough disorder in the substrate for effective proteasomal degradation. To study whether Fat10ylation at multiple sites has a higher effect, we conjugated Ube2z with Fat10 at all three sites simultaneously. The conformational entropy was increased by 0.8 kcal/mol per residue, suggesting higher disorder upon multi-monoFat10ylation.

The loss of native and side-chain contacts in Ube2z was lower than in Parkin-Ubl (Figure 5d(i),(ii)). While Parkin-Ubl had up to a 20% loss in native contacts upon Fat10ylation, Ube2z showed only ∼8% loss of backbone native contacts. Similarly, while Parkin-Ubl had up to 45% loss in native side-chain contacts, Ube2z had a 25% loss of side-chain native contacts. The more significant loss in native contacts correlates with the more remarkable change in conformational entropy observed in Parkin-Ubl. Within the lysines of Ube2z, more side-chain native contacts were disrupted when Fat10 was conjugated to K238 compared to the other two lysines. Simultaneous with the disruption of native contacts, new non-native backbone and side-chain contacts were formed between Fat10 and the substrate (Figure 5d(iii),(iv)). To examine the substrate regions contacted by Fat10, we plotted the contacts

https://doi.org/10.1021/acsomega.4c01396
ACS Omega 2024, 9, 22265−22276

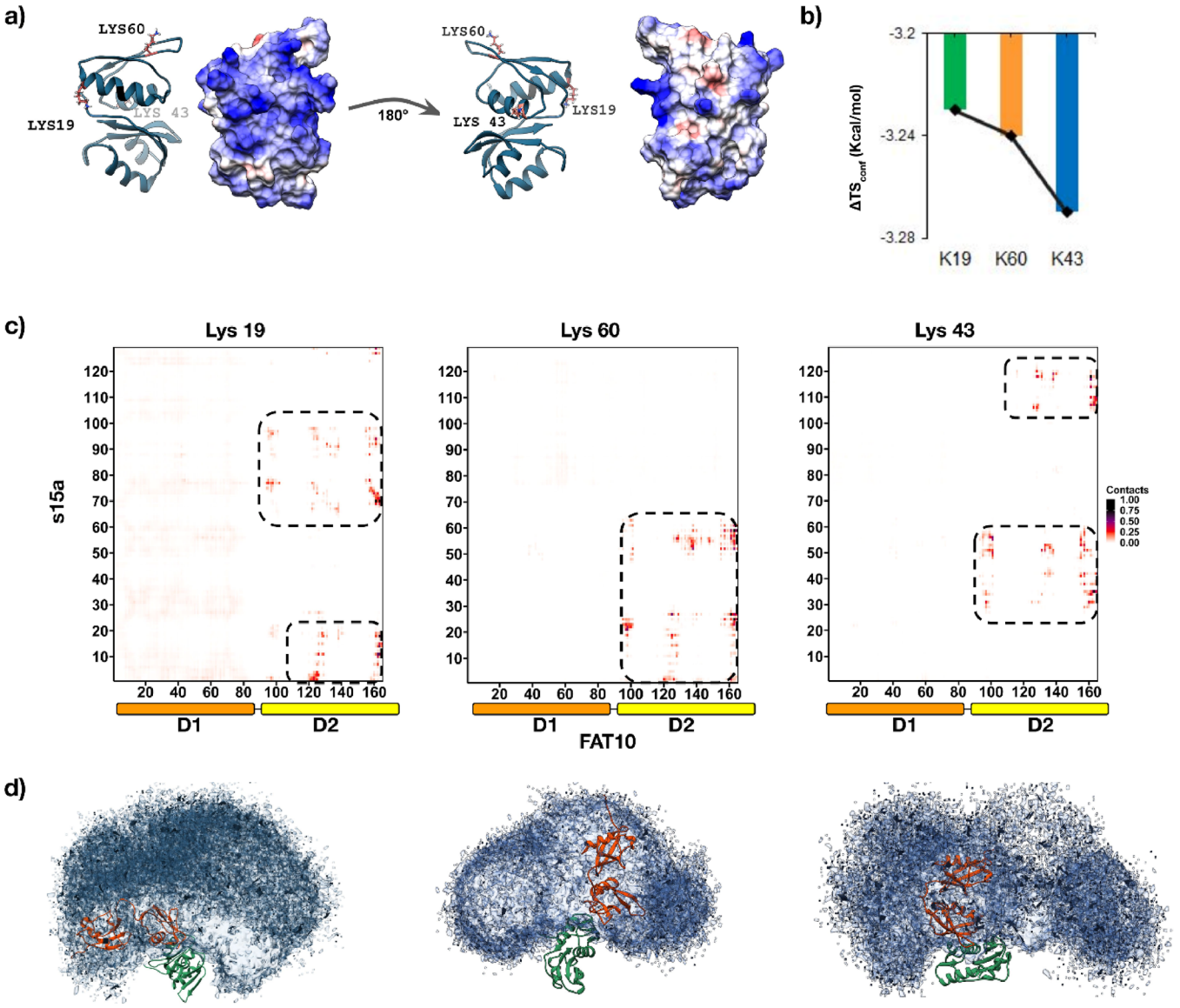

Figure 6. The effect of Fat10 on s15a was studied by MD simulations. (a) Surface of the s15a domain mapped by electrostatic coloring. Three lysine residues used for Fat10 conjugation are shown. (b) The conformational entropic contributions to the free energy are plotted for the three sites. (c) Contact maps plotted for the intermolecular contacts between Fat10 and s15a for all three sites. The area within the broken black lines shows the contacts near the Fat10ylation site. (d) The occupancy of Fat10 in the s15a∼Fat10 conjugate is plotted. The s15a molecule is colored green, and Fat10 is colored orange. s15a was kept fixed, and the occupancy of Fat10 around s15a is shown in blue.

between Fat10 and the substrate as contact maps (Figure 5e). In K130 and K186 Fat10ylations, contacts were restricted to near conjugation sites. No contacts were observed between the D1 domain and the substrate in these cases. K238 Fat10ylation had more intermolecular contacts between Fat10 and Ube2z, commensurate with its slightly higher ΔTS_{conf} values.

We then mapped the surface electrostatics of the Fat10-Ube2z conjugates. The top three cluster representatives for all conjugates are shown in Figure S9. Three long disordered regions provide the interdomain conformational flexibility in Fat10: (i) the N-terminal tail, (ii) the linker between N- and C-termini, and (iii) the C-terminal tail. Since Fat10 is conjugated via the C-terminal end, the dynamics of the C-terminal tail and the linker region may have a prominent role in Fat10's conformational dynamics in the conjugate. K130 and K186 are present in the positively charged patch of Ube2z, which complements the C-terminal negatively charged D2 patch (Figure S10), creating a strong local interaction that restricts C-terminal tail conformational dynamics and reduces nonspecific interactions between the Fat10 D1 domain and the substrate. On the other hand, K238 is present in a negatively charged region, which repels the D2 domain and enhances the conformational dynamics in Fat10 and the interactions of the D1 domain with the substrate.

Surface Electrostatics at the Conjugation Site Modulates the Substrate Energy. To study if the conjugation site can modulate the effect of Fat10ylation, we chose s15a (20 kDa), a subunit of the 40S ribosomal complex, as another test substrate.[24] s15a Fat10ylation suggests a role of the Fat10-proteasome pathway in protein translation. We chose three lysines in the protein: Lys19, Lys60, and Lys43. Lys19 is present in helix α1, Lys60 in strand β3, and Lys43 in helix α1. Lys19 and Lys60 are located within the positively charged surface patch in s15a (Figure 6a). However, Lys43 is

https://doi.org/10.1021/acsomega.4c01396
ACS Omega 2024, 9, 22265−22276

present in the negatively charged surface patch. The effect of Fat10 conjugation on the conformational entropy is ∼3.2 kcal/mol/residue, where Lys43 showed slightly higher negative ΔTS_{conf} values (Figure 6b). While the contact map shows that the interaction of FAT10 is restricted to D2, D1 does not form any stable contacts with the substrate (Figure 6c). We also examined the nature of surface interactions between Fat10 and s15a by analyzing the top three representative clusters from the simulations and the occupancy map of Fat10 (Figure 6d and Figure S11). s15a has a considerably positively charged patch on the surface, and conjugation in the patch creates a strong interaction interface between s15a and the negatively charged D2 domain in Fat10. The effect is less in Lys43, which is located at a negatively charged surface, leading to a larger occupancy surface (Figure 6d). These strong local interactions between Fat10 and the substrate limit the conformational dynamics of Fat10 and therefore decrease the interaction of the Fat10 N-terminal domain with the substrate.

DISCUSSION

The Fat10-proteasome pathway is upregulated in response to inflammation and plays a crucial role in modulating the immune response. However, the mechanisms underlying substrate degradation in the pathway have been poorly defined. Modification of substrates with Fat10 targets their degradation by the proteasome. At the proteasome, the substrate and Fat10 are unfolded mechanically by ATPase before entering the core particle. Recent studies have suggested that the N-terminal disordered region in Fat10 is relevant for substrate degradation,[25] suggesting that Fat10 may first enter the proteasome core by N-terminal mechanical pulling by the ATPase, followed by the substrate. We studied the unfolding pathway in Fat10 by N-terminal mechanical pulling, which revealed that the long-range contacts between N-terminal β-strand 1 and other adjacent contacts are initially disrupted in domain 1 in Fat10. Subsequently, the central α-helix dissociates from the α-sheet, and the secondary structures unfold. Domain 2 unfolds successively in a similar sequence of events. For substrates with significant inherent disorder, it cannot be ruled out that the disordered substrate enters the ATPase first, followed by Fat10. In such a case, Fat10 is pulled along the C-terminus. We find that the sequence of unfolding events in Fat10 is similar for pulling from either the N- or C-terminus. However, the N-terminal pulling required less work, suggesting that the Fat10-enters-first pathway may be the preferred pathway. Notably, the structural details of the Fat10/receptor interaction at the proteasome are unknown and excluded in the current analysis. We then studied the substrate's mechanical unfolding pathway, which suggested that the unfolding pathway and work required to unfold the substrate depend on the site of Fat10ylation.

Partial disorder in substrates is essential for effective proteasomal degradation.[26] Proteasome degradation tags like ubiquitin increase disorder and modulate the energetics of its substrates depending on the site of conjugation.[11,12,27,28] Although Fat10ylation enhances substrate disorder,[13] its site-specific effects are unclear. Fat10 also targets a range of substrates with differences in sizes and flexibilities.[8] The impact of Fat10ylation on the thermodynamic properties of different substrates is unknown. Here, we explored the impact of Fat10ylation on the thermodynamic properties of substrates with various sizes and inherent flexibilities. Our findings indicate that Fat10ylation induces an entropic destabilization of the substrate's native state. The quantum of destabilization depends on a variety of factors. Smaller substrates exhibit a more pronounced response to Fat10lylation compared with larger substrates. Larger substrates may need multi-mono-Fat10ylation for effective degradation. Fat10ylated heteromers or oligomers must dissociate before they are degraded at the proteasome. It would be interesting to study the effect of Fat10 on the interprotomer interactions in such heteromers/oligomers. We also uncovered that rigid substrates have a reduced effect of Fat10ylation compared to flexible or partially disordered substrates. Conjugation with proteasome targeting tags does not guarantee degradation, as the substrates may escape the proteasome in the absence of sufficient disorder,[26] a regulatory mechanism postulated to prevent aberrant degradation. The susceptibility of distinct substrates to specific levels of disorder upon Fat10ylation may prevent aberrant degradation of the Fat10-proteasome pathway.

Like ubiquitin,[29] Fat10 destabilizes the substrate's native state by reducing the conformational entropy. Fat10 is attached to substrates via a peptide bond between the C-terminal glycine of Fat10 and the Nζ of a lysine residue on the substrate. Our findings suggest that the effect of Fat10 varies depending on the conformational landscape surrounding the substrate, which, in turn, relies on the site of Fat10ylation. The C-terminal tail of Fat10 is flexible, which enables it to explore a wide range of conformational landscapes around the substrate. However, strong interactions between Fat10 and the substrate at the Fat10ylation site limit the motion of the C-terminal tail of Fat10 and the conformational landscape. Interestingly, the C-terminal region of Fat10 includes a negatively charged surface (Figure S10). If the substrate has a significantly positively charged surface near the Fat10ylation site, then it creates strong local electrostatic interactions with the negatively charged surface in the Fat10 C-terminal region, restricting the movement of Fat10 and its impact on the substrate energetics.

Substrates of the Fat10-proteasome pathway are degraded rapidly and do not require unfoldases like VCP/p97,[13] thereby suggesting an attractive mechanism for targeted degradation using proteolysis-targeting chimera (PROTAC). An identified E3 for Fat10 modification is Parkin, which could be used for such purpose.[30] However, the modalities of PROTAC design for Fat10 need further insights, including identifying suitable heterobifunctional molecules and the sites of substrate modification. Our findings suggest that Fat10 should be incorporated at negatively charged or neutral surfaces of the substrate for more effective degradation.

CONCLUSIONS

We studied how Fat10ylation affects substrate thermodynamic stability, considering substrate size, surface charge, and flexibility, to provide mechanistic insights into the Fat10-proteasome pathway. Our comprehensive analysis has provided detailed insights into the effects of Fat10ylation on substrate thermodynamic stability and conformational flexibility. The findings indicate that Fat10ylation significantly reduces the thermodynamic stability of substrates while increasing their conformational flexibility. Moreover, Fat10's effect on the entropy of the Fat10-substrate conjugate is consistent across different regions. However, the degree of entropic change varies depending on the size of the substrate. Fat10ylation has a more significant effect on the conformational entropy of smaller substrates than on larger substrates.

https://doi.org/10.1021/acsomega.4c01396
ACS Omega 2024, 9, 22265−22276

Furthermore, our analysis has shown that the impact of Fat10 on the entropy of substrates is closely related to their intrinsic flexibility. Fat10 has a more significant effect on the entropy of intrinsically flexible substrates than that of rigid substrates. Finally, our results also suggest that the difference in entropy depends on the conformational landscape of Fat10. If Fat10 interacts with the substrate in a stable and specific manner at the modification site, then it reduces Fat10's destabilizing effect by reducing its conformational flexibility. Fat10ylation modulates substrate stability by entropic destabilization, and the change in entropy depends on substrate size, the substrate's intrinsic flexibility, and the site of Fat10 modification.

MATERIALS AND METHODS

System Preparation. The structures for individual domains of Fat10D1 and Fat10D2 were retrieved from PDB IDs 6GF1 and 6GF2, respectively.[10] The full-length Fat10 structure was modeled using Swiss-Modeler[31] with 6GF1 and 6GF2 templates. Chain B of 6GF1 was further processed for simulation, and it is called Fat10D1. All water and sulfate molecules were removed from the Fat10D1 crystal structure. 6GF2 was an NMR ensemble structure, and the best representative structure, Fat10D2, was further considered for simulation. The structures for the ubiquitin-like (Ubl) domain of Parkin, UBE2Z, and s15a were retrieved from PDB IDs 1IYF, 5A4P, and 6ZMI, respectively. All water, ions, and small molecules were removed from the crystal structures. The Fat10-substrate complex was made by adding an isopeptide bond between the Fat10 terminal glycine and respective Lys from substrates. The best representative structure of the Ubl domain of Parkin from the NMR models was Fat10ylated at Lys32, Lys48, and Lys76. The s15a structure was isolated from 6ZMI and was Fat10ylated at Lys19, Lys43, and Lys60. Ube2z was Fat10ylated at Lys130, Lys186, and Lys238. Systems for Fat10, substrates, and Fat10-substrate complex were prepared with the LEaP program of Ambertools18.[32,33] Systems were designed in a cubic box of TIP3p water, with a minimum distance of at least 12 Å between solute atoms and the box edge. Counterions were added to neutralize the system. Isopeptide bonds were parametrized as in a previous study.[34]

MD Simulation. Parameters describing the system topology were based on the Amber ff99SBildn force field. The systems were first relaxed by energy minimization in two stages by using the Sander module of Amber18. In the first stage, water molecules were minimized with restraint on protein, and then the entire system was minimized. The respective systems were then heated incrementally in NVT from 0 to 300 K for 5 ns with positional restraints (20 kcal/mol/Å^2) on protein atoms. Further, system density was equilibrated for 5 ns in the NPT ensemble with positional restraints (20 kcal/mol/Å^2) on protein atoms. Additionally, four subsequent equilibration stages reduced the restraints on the backbone atom from 20 to 0 through a series of molecular dynamics simulations in an NPT ensemble of 400 ps each. The final production run was performed for 1 μs in NPT with three replicas. The distance cutoff for short-range nonbonded interactions was set to 1 nm. The particle mesh Ewald (PME) method was used to treat long-range electrostatic interactions. The SHAKE algorithm was applied to constrain all bonds involving hydrogen atoms. The temperature was set to 300 K using a Langevin thermostat, and pressure was maintained at 1 bar using the Berendsen barostat. Using the hydrogen mass repartitioning (HMR) scheme,[35] the integration time step was set to 4 fs. Dynamics were propagated using the leapfrog integrator. Snapshots were saved every 40 ps, giving 25,000 conformations from a single run. A total of 3 μs (3 × 1 μs) data were pooled for further analysis.

Pulling Simulations. ASMD simulations were performed by taking Jarzynski's average at small intervals of reaction coordinates.[36,37] Constant force implicit solvent ASMD simulations of the unfolding of Fat10 and the Ubl domain of Parkin were carried out. Fat10 was pulled from its N-terminus with 100 kcal positional restraint on the C-terminus. For Ubl, the system was pulled from its Lys residues with positional restraints of the termini for Lys32 and Lys48, whereas only the N-terminal restraint was used for Lys72.

The reaction coordinate is the end-to-end distance between the CA atoms of the respective protein's first and last amino acids. Simulations were pulled at a constant 10 Å/ns velocity. The reaction coordinate is partitioned into five equal segments (100, 26, 24, and 45 Å in length for Fat10, Ubl-Lys32, Ubl-Lys48, and Ubl-Lys76, respectively) with 15 trajectories per segment. The system was energy-minimized and equilibrated, and the resulting coordinates and velocities were used as starting points for the ASMD simulations. Nonbonded interactions were treated with a cutoff of 999 Å.

MD Analysis. The trajectories were analyzed using the CPPTRAJ[38] module in the AMBER suite. Further, the averages and standard errors were calculated using in-house scripts and plotted using the R program.

Native Contacts. Native contacts were calculated using the native contact method present in CPPTRAJ with a 7.0 Å distance cutoff. For backbone native contacts across secondary structure pairs, the native contacts were calculated, defining a 3.5 Å distance cutoff on backbone atoms.

Entropy Calculation. Configurational entropic contributions to the free energy (normalized by the number of residues in the substrate, kcal/mol) in Fat10ylated and unmodified substrates were determined. Calculations were performed based on covariance matrices of the atomic fluctuations observed in the MD trajectories. MMPBSA.py was used with the "Stability" option with receptor and ligand prmtop options blank.[39] The configurational entropy is the average of the independent entropies independently estimated for each run. The configurational entropy was assessed using the quasi-harmonic approximation. The change in conformational entropy due to Fat10ylation was calculated using

$$\Delta TS_{\text{Fat10ylation}} = \Delta TS_{\text{Fat10}\sim\text{substrate}} - (\Delta TS_{\text{Fat10}} + \Delta TS_{\text{substrate}})$$

Occupancy Plots. Occupancy values of Fat10 were computed using the substrate atoms as a reference set of atoms, employing UCSF Chimera. These occupancy values indicate the frequency with which atoms within the specified set fall into a grid cell. Volumetric grids of this nature were utilized to visualize the movement of Fat10 around the substrate across three replica trajectories. The structure shown in the occupancy data serves as a reference to illustrate the relative orientation of Fat10 with respect to the substrate.

Clustering and Cluster Representatives. Cluster representatives were determined using the NMRCLUST algorithm. This algorithm circumvents the need for predefined cutoffs to determining clusters. This algorithm is part of UCSF Chimera, and it was used for cluster calculations.

https://doi.org/10.1021/acsomega.4c01396
ACS Omega 2024, 9, 22265−22276

■ ASSOCIATED CONTENT

Supporting Information

The Supporting Information is available free of charge at https://pubs.acs.org/doi/10.1021/acsomega.4c01396?goto=-supporting-info.

Pulling snapshots, pathways, contact maps, electrostatic surface representations, Fat10ylation table, etc. (PDF)

Trajectory of Fat10 pulling from N-terminal and C-terminal ends (MP4)

■ AUTHOR INFORMATION

Corresponding Author

Ranabir Das − *National Center for Biological Sciences, Tata Institute of Fundamental Research, Bangalore 560065, India;* orcid.org/0000-0001-5114-6817; Email: rana@ncbs.res.in

Author

Aravind Ravichandran − *National Center for Biological Sciences, Tata Institute of Fundamental Research, Bangalore 560065, India; SASTRA University, Thanjavur 613401, India;* orcid.org/0000-0003-1701-5535

Complete contact information is available at: https://pubs.acs.org/10.1021/acsomega.4c01396

Author Contributions

A.R. and R.D. designed the study. A.R. carried out all simulations and data analysis. R.D. supervised the project and acquired funds. A.R. wrote the initial manuscript draft. Both authors contributed to the final draft.

Notes

The authors declare no competing financial interest.

■ ACKNOWLEDGMENTS

This work was supported by the Tata Institute of Fundamental Research, Department of Atomic Energy, Government of India, under project identification no. RTI 4006. A.R. acknowledges scholarships from the Department of Biotechnology, India.

■ REFERENCES

(1) Sha, Z.; Zhao, J.; Goldberg, A. L. Measuring the Overall Rate of Protein Breakdown in Cells and the Contributions of the ubiquitin-Proteasome and Autophagy-Lysosomal Pathways. *Methods Mol. Biol.* **2018**, *1844*, 261−276.

(2) Goldberg, A. L.; Kim, H. T.; Lee, D.; Collins, G. A. Mechanisms That Activate 26s Proteasomes and Enhance Protein Degradation. *Biomolecules* **2021**, *11* (6). 779.

(3) McCarthy, M. K.; Weinberg, J. B. The Immunoproteasome and Viral Infection: A Complex Regulator of Inflammation. *Front. Microbiol.* **2015**, *6* (JAN), 1−16.

(4) Çetin, G.; Klafack, S.; Studencka-Turski, M.; Krüger, E.; Ebstein, F. The ubiquitin−Proteasome System in Immune Cells. *Biomolecules* **2021**, *11* (1), 60−23.

(5) Mao, Y. Structure, Dynamics and Function of the 26S Proteasome. *Subcell. Biochem.* **2021**, *96*, 1−151.

(6) Basler, M.; Buerger, S.; Groettrup, M. The ubiquitin-like Modifier FAT10 in Antigen Processing and Antimicrobial Defense. *Mol. Immunol.* **2015**, 129−13.

(7) Aichem, A.; Groettrup, M. The ubiquitin-like Modifier FAT10 - Much More than a Proteasome-Targeting Signal. *J. Cell Sci.* **2020**, *133* (14), No. jcs246041, DOI: 10.1242/jcs.246041.

(8) Leng, L.; Xu, C.; Wei, C.; Zhang, J.; Liu, B.; Ma, J.; Li, N.; Qin, W.; Zhang, W.; Zhang, C.; Xing, X.; Zhai, L.; Yang, F.; Li, M.; Jin, C.; Yuan, Y.; Xu, P.; Qin, J.; Xie, H.; He, F.; Wang, J. A Proteomics Strategy for the Identification of FAT10-Modified Sites by Mass Spectrometry. *J. Proteome Res.* **2014**, *13* (1), 268−276.

(9) Schmidtke, G.; Aichem, A.; Groettrup, M. FAT10ylation as a Signal for Proteasomal Degradation. *Biochim. Biophys. Acta - Mol. Cell Res.* **2014**, *1843* (1), 97−102.

(10) Aichem, A.; Anders, S.; Catone, N.; Rößler, P.; Stotz, S.; Berg, A.; Schwab, R.; Scheuermann, S.; Bialas, J.; Schütz-Stoffregen, M. C.; Schmidtke, G.; Peter, C.; Groettrup, M.; Wiesner, S. The Structure of the ubiquitin-like Modifier FAT10 Reveals an Alternative Targeting Mechanism for Proteasomal Degradation. *Nat. Commun.* **2018**, *9* (1), 3321 DOI: 10.1038/s41467-018-05776-3.

(11) Carroll, E. C.; Latorraca, N. R.; Lindner, J. M.; Maguire, B. C.; Pelton, J. G.; Marqusee, S. Mechanistic Basis for ubiquitin Modulation of a Protein Energy Landscape. *Proc. Natl. Acad. Sci. U. S. A.* **2021**, *118* (12), 126a DOI: 10.1073/pnas.2025126118.

(12) Carroll, E. C.; Greene, E. R.; Martin, A.; Marqusee, S. Site-Specific Ubiquitination Affects Protein Energetics and Proteasomal Degradation. *Nat. Chem. Biol.* **2020**, *16* (8), 866−875.

(13) Negi, H.; Ravichandran, A.; Dasgupta, P.; Reddy, S.; Das, R. Plasticity of the Proteasome-Targeting Signal Fat10 Enhances Substrate Degradation. *bioRxiv* **2023**, DOI: 10.1101/2022.07.15.499953.

(14) Roverato, N. D.; Sailer, C.; Catone, N.; Aichem, A.; Stengel, F.; Groettrup, M. Parkin Is an E3 Ligase for the ubiquitin-like Modifier FAT10, Which Inhibits Parkin Activation and Mitophagy. *Cell Rep.* **2021**, *34* (11), No. 108857.

(15) Aichem, A.; Catone, N.; Groettrup, M. Investigations into the Auto-FAT10ylation of the Bispecific E2 Conjugating Enzyme UBA6-Specific E2 Enzyme 1. *FEBS J.* **2014**, *281* (7), 1848−1859.

(16) Das, A.; Mukhopadhyay, C. Mechanical Unfolding Pathway and Origin of Mechanical Stability of Proteins of ubiquitin Family: An Investigation by Steered Molecular Dynamics Simulation. *Proteins Struct. Funct. Bioinforma.* **2009**, *75* (4), 1024−1034.

(17) Li, P. C.; Makarov, D. E. Simulation of the Mechanical Unfolding of ubiquitin: Probing Different Unfolding Reaction Coordinates by Changing the Pulling Geometry. *J. Chem. Phys.* **2004**, *121*, 4826−4832.

(18) EMBO Reports - 2003 - Sakata - Parkin Binds the Rpn10 Subunit of 26S Proteasomes through Its ubiquitin-like Domain.Pdf.

(19) Schelpe, J.; Monté, D.; Dewitte, F.; Sixma, T. K.; Rucktooa, P. Structure of UBE2Z Enzyme Provides Functional Insight into Specificity in the FAT10 Protein Conjugation Machinery. *J. Biol. Chem.* **2016**, *291* (2), 630−639.

(20) Aichem, A.; Pelzer, C.; Lukasiak, S.; Kalveram, B.; Sheppard, P. W.; Rani, N.; Schmidtke, G.; Groettrup, M. USE1 Is a Bispecific Conjugating Enzyme for ubiquitin and FAT10, Which FAT10ylates Itself in Cis. *Nat. Commun.* **2010**, *1* (2), 1−10.

(21) Das, R.; Mariano, J.; Tsai, Y. C.; Kalathur, R. C.; Kostova, Z.; Li, J.; Tarasov, S. G.; McFeeters, R. L.; Altieri, A. S.; Ji, X.; Byrd, R. A.; Weissman, A. M. Allosteric Activation of E2-RING Finger-Mediated Ubiquitylation by a Structurally Defined Specific E2-Binding Region of Gp78. *Mol. Cell* **2009**, *34* (6), 674−685.

(22) Das, R.; Liang, Y. H.; Mariano, J.; Li, J.; Huang, T.; King, A.; Tarasov, S. G.; Weissman, A. M.; Ji, X.; Byrd, R. A. Allosteric Regulation of E2:E3 Interactions Promote a Processive Ubiquitination Machine. *EMBO J.* **2013**, *32* (18), 2504−2516.

(23) Houben, K.; Dominguez, C.; van Schaik, F. M. A.; Timmers, H. T. M.; Bonvin, A. M. J. J.; Boelens, R. Solution Structure of the ubiquitin-Conjugating Enzyme UbcH5B. *J. Mol. Biol.* **2004**, *344* (2), 513−526.

(24) Aichem, A.; Kalveram, B.; Spinnenhirn, V.; Kluge, K.; Catone, N.; Johansen, T.; Groettrup, M. The Proteomic Analysis of Endogenous FAT10 Substrates Identifies P62/SQSTM1 as a Substrate of FAT10ylation. *J. Cell Sci.* **2012**, *53*, 4576−4585.

(25) Aichem, A.; Anders, S.; Catone, N.; Rößler, P.; Stotz, S.; Berg, A.; Schwab, R.; Scheuermann, S.; Bialas, J.; Schütz-Stoffregen, M. C.; Schmidtke, G.; Peter, C.; Groettrup, M.; Wiesner, S. The Structure of the ubiquitin-like Modifier FAT10 Reveals an Alternative Targeting

Mechanism for Proteasomal Degradation. *Nat. Commun.* **2018**, *9* (1), 1−14.
(26) Correa Marrero, M.; Barrio-Hernandez, I. Toward Understanding the Biochemical Determinants of Protein Degradation Rates. *ACS Omega* **2021**, *6* (8), 5091−5100.
(27) Morimoto, D.; Walinda, E.; Fukada, H.; Sugase, K.; Shirakawa, M. Ubiquitylation Directly Induces Fold Destabilization of Proteins. *Sci. Rep.* **2016**, *6*, 39453 DOI: 10.1038/srep39453.
(28) Hagai, T.; Levy, Y. ubiquitin Not Only Serves as a Tag but Also Assists Degradation by Inducing Protein Unfolding. *Proc. Natl. Acad. Sci. U. S. A.* **2010**, *107* (5), 2001−2006.
(29) Gavrilov, Y.; Hagai, T.; Levy, Y. Nonspecific yet Decisive: Ubiquitination Can Affect the Native-State Dynamics of the Modified Protein. *Protein Sci.* **2015**, *24* (10), 1580−1592.
(30) Roverato, N. D.; Sailer, C.; Catone, N.; Aichem, A.; Stengel, F.; Groettrup, M. Parkin Is an E3 Ligase for the ubiquitin-like Modifier FAT10, Which Inhibits Parkin Activation and Mitophagy. *Cell Rep.* **2021**, *34* (11). 108857.
(31) Waterhouse, A.; Bertoni, M.; Bienert, S.; Studer, G.; Tauriello, G.; Gumienny, R.; Heer, F. T.; De Beer, T. A. P.; Rempfer, C.; Bordoli, L.; Lepore, R.; Schwede, T. SWISS-MODEL: Homology Modelling of Protein Structures and Complexes. *Nucleic Acids Res.* **2018**, *46* (W1), W296−W303.
(32) Tian, C.; Kasavajhala, K.; Belfon, K. A. A.; Raguette, L.; Huang, H.; Migues, A. N.; Bickel, J.; Wang, Y.; Pincay, J.; Wu, Q.; Simmerling, C. Ff19SB: Amino-Acid-Specific Protein Backbone Parameters Trained against Quantum Mechanics Energy Surfaces in Solution. *J. Chem. Theory Comput.* **2020**, *16* (1), 528−552.
(33) Case, D. A.; Ben-Shalom, I. Y.; Brozell, S. R.; Cerutti, D. S.; Cheatham, T. E.; III, V. W. D. C.; Darden, T. A.; Duke, R. E.; Ghoreishi, D.; Gilson, M. K.; Gohlke, H.; Goetz, A. W.; Greene, D.; Harris, R.; Homeyer, N.; Izadi, S.; Kovalenko, A.; Kurtzman, T.; Lee, T. S.; LeGrand, S.; Li, P.; Lin, C.; Liu, J.; Luchko, T.; Luo, R.; Mermelstein, D. J.; Merz, K. M.; Miao, Y.; Monard, G.; Nguyen, C.; Nguyen, H.; Omelyan, I.; Onufriev, A.; Pan, F.; Qi, R.; Roe, D. R.; Roitberg, A.; Sagui, C.; Schott-Verdugo, S.; Shen, J.; Simmerling, C. L.; Smith, J.; Salomon-Ferrer, R.; Swails, J.; Walker, R. C.; Wang, J.; Wei, H.; Wolf, R. M.; Wu, X.; Xiao, L.; York, D. M.; Kollman, P. A. *Amber18*; Univ. California: San Fr. 2018.
(34) Mark, P.; Nilsson, L. Structure and Dynamics of the TIP3P, SPC, and SPC/E Water Models at 298 K. *J. Phys. Chem. A* **2001**, *105*, 9954−9960.
(35) Hopkins, C. W.; Le Grand, S.; Walker, R. C.; Roitberg, A. E. Long-Time-Step Molecular Dynamics through Hydrogen Mass Repartitioning. *J. Chem. Theory Comput.* **2015**, *11* (4), 1864−1874.
(36) Truong, D. T.; Li, M. S. Probing the Binding Affinity by Jarzynski's Nonequilibrium Binding Free Energy and Rupture Time. *J. Phys. Chem. B* **2018**, *122* (17), 4693−4699.
(37) Mücksch, C.; Urbassek, H. M. Accelerating Steered Molecular Dynamics: Toward Smaller Velocities in Forced Unfolding Simulations. *J. Chem. Theory Comput.* **2016**, *12* (3), 1380−1384.
(38) Roe, D. R.; Cheatham, T. E. PTRAJ and CPPTRAJ: Software for Processing and Analysis of Molecular Dynamics Trajectory Data. *J. Chem. Theory Comput.* **2013**, *9* (7), 3084−3095.
(39) Miller, B. R.; McGee, T. D.; Swails, J. M.; Homeyer, N.; Gohlke, H.; Roitberg, A. E. Py: An Efficient Program for End-State Free Energy Calculations. *J. Chem. Theory Comput.* **2012**, *8* (9), 3314−3321.

https://doi.org/10.1021/acsomega.4c01396
ACS Omega 2024, 9, 22265−22276